Anionic Group 6 Metal Carbonyl Oxalate Complexes. X-ray Structures of $[Et_4N]_2[W(CO)_4C_2O_4]$ and $[PPN]_2[W_2(CO)_8C_2O_4]\cdot{}^1/_2(CH_3CH_2)_2O$

Donald J. Darensbourg,* Jennifer A. Chojnacki, and Joseph H. Reibenspies

Department of Chemistry, Texas A&M University, College Station, Texas 77843

Received January 17, 1992

The reaction of the oxalate anion, $C_2O_4^{2-}$, with $W(CO)_5$(solvent) results in rapid formation of $W(CO)_4(\eta^2\text{-}C_2O_4)^{2-}$ (**1**). On the basis of kinetic parameters previously determined for a series of $W(CO)_5O_2CR^-$ derivatives, complexes containing a carboxylate ligand with a good electron-releasing group, R, are subject to facile displacement of a cis CO. Indeed, in the case of the predicted initial product, $W(CO)_5(\eta^1\text{-}C_2O_4)^{2-}$, this displacement is anticipated to occur readily, as was observed, with $t_{1/2}$ = 23 s. Complex **1** reacts with a second molecule of $W(CO)_5$(solvent) to form the stable dimer $W_2(CO)_8(\eta^2\text{-}C_2O_4)^{2-}$ (**2**). Additionally, the dimeric species can be formed directly from $W(CO)_5$(solvent) + $^1/_2C_2O_4^{2-}$. This reaction initially gives $W_2(CO)_{10}(\eta^1\text{-}C_2O_4)^{2-}$, from which **2** can be produced by removal of two labile CO molecules. The X-ray structures of $[Et_4N]_2$[**1**] and $[PPN]_2$[**2**]$\cdot{}^1/_2(CH_3CH_2)_2O$ are reported. The complex $[Et_4N]_2$[**1**] crystallizes in the monoclinic space group $P2_1/n$ with a = 8.581 (5) Å, b = 24.773 (9) Å, c = 13.151 (5) Å, β = 108.56 (3)°, V = 2650 (2) Å^3, and Z = 4. Refinement converged at R = 5.51% and R_w = 4.70% for those 2890 reflections with $F > 4.0\sigma(F)$ at T = 193 K. The complex $[PPN]_2$[**2**]$\cdot{}^1/_2(CH_3CH_2)_2O$ crystallizes in the monoclinic space group $P2_1/c$ with a = 14.745 (7) Å, b = 12.916 (4) Å, c = 20.415 (9) Å, β = 95.60 (4)°, V = 3869 (3) Å^3, and Z = 2. Refinement converged at R = 6.47% and R_w = 6.08% for those 4695 reflections with $F > 4.0\sigma(F)$ at T = 193 K.

Introduction

In our comprehensive efforts to understand the organometallic chemistry of carbon dioxide, we have been concerned with the role of metal unsaturation in the decarboxylation mechanism of $M(CO)_5O_2CR^-$ derivatives.[1-3] Associated with this, the function of neighboring-group participation in CO substitution reactions of group 6 metal carboxylates has been investigated (eq 1)[4] and

$$W(CO)_5O_2CR^- + PR'_3 \rightarrow \textit{cis}\text{-}W(CO)_4[O_2CR](PR'_3) + CO \quad (1)$$

the rate of *cis*-CO group substitution found to be promoted by electron-releasing R substituents. For example, the rate constant for CO loss in the pivalate derivative (R = $-C(CH_3)_3$, σ^* = −0.30) is 10.9×10^{-3} s^{-1} at 40 °C, whereas the corresponding rate constant for the cyanoacetate derivative (R = $-CH_2CN$, σ^* = 1.30) is 0.744×10^{-3} s^{-1}.

Since the value of Taft's polar substituent constant, σ^*, in the oxalate ligand (i.e., R = CO_2^-) is −1.06, it is anticipated that the $W(CO)_5(\eta^1\text{-}C_2O_4)^{2-}$ derivative would undergo facile CO substitution. This presentation represents an investigation of the interactions of the $C_2O_4^{2-}$ ligand with photogenerated $[W(CO)_5]$ and the subsequent reactions of the resulting complex. In addition, this chemistry is of general interest in the area of CO_2 activation. That is, complexes analogous to those described herein could arise from the head-to-head coupling of electrochemically or chemically generated $CO_2^{\bullet-}$ species upon subsequent binding of the resultant oxalate ligand to a metal center.[5]

Experimental Section

Materials. All manipulations were carried out in either an argon-filled drybox or on a double-manifold Schlenk vacuum line. Solvents were dried by standard methods and distilled under a nitrogen atmosphere prior to use. Chemical reagents were commercially available and were used without further purification. Experiments utilizing photolysis were performed with a 450-W mercury arc UV immersion lamp purchased from Ace Glass Co. Infrared spectra were recorded on an IBM FTIR/32 spectrometer or on an IBM FTIR/85 spectrometer using a 0.1-mm NaCl solution cell. NMR spectra were taken on a Varian XL-200 superconducting high-resolution spectrometer with an internal deuterium lock in 5-mm tubes.

Synthesis of $[Et_4N]_2[C_2O_4]$. To a solution of HO_2CCO_2H (3.0 g, 33.3 mmol, in 50 mL of deionized H_2O) was added Et_4NOH (39.3 g, 66.7 mmol, 25% by weight in methanol) via syringe. The solution was stirred for several minutes, and the solvent was removed under reduced pressure to afford a viscous liquid. The product was washed six times with diethyl ether and dried in a vacuum oven at 60 °C for 12–18 h to give a white powder in 65% yield. The product was very hygroscopic and was therefore stored in the drybox.

Synthesis of $[Et_4N]_2[W(CO)_4(\eta^2\text{-}O_2CCO_2)]$ ($[Et_4N]_2$[1**]).** A solution of $W(CO)_6$ (0.447 g, 1.27 mmol, in 65 mL of CH_3CN) was placed in a water-jacketed photolysis vessel, and a vigorous stream of nitrogen was bubbled through the solution. After 25 min of photolysis, the infrared spectrum indicated a mixture of $W(CO)_5CH_3CN$ and *cis*-$W(CO)_4(CH_3CN)_2$. The yellow photoproduct was added slowly to a solution of $[Et_4N]_2[C_2O_4]$ (0.443 g, 1.27 mmol, in 20 mL of CH_3CN) over a period of 20 min while the flask was warmed with a 40 °C water bath. The orange solution was heated at 50 °C and stirred for 6 h; infrared spectroscopy indicated complete conversion to the disubstituted mononuclear product. The solution was filtered through Celite and concentrated under reduced pressure. Addition of diethyl ether resulted in precipitation of an orange oil. The product was washed three times with 20-mL portions of ether and recrystallized from acetonitrile and diethyl ether. Thorough washing with ether afforded a yellow powder: 56% yield; IR (CH_3CN) ν_{CO} 1986 (w), 1847 (s), 1825 (sh), 1782 (s) cm^{-1}; IR (CH_3CN) ν_{COO} 1658 (s) cm^{-1}; ^{13}C NMR (CD_3CN) 218.2 (s), 205.4 (s) ppm. Anal. Calcd for $WC_{22}H_{40}O_8N_2$: C, 41.0; H, 6.3. Found: C, 37.5; H, 6.3. X-ray-quality crystals were produced by low-temperature crystallization from acetonitrile/diethyl ether. An infrared spectrum of the crystals in acetonitrile was identical to that of the bulk product.

Synthesis of $[Et_4N]_2[W_2(CO)_8(\eta^2\text{-}O_2CCO_2)]$. To a solution of $[Et_4N]_2[W(CO)_4(\eta^2\text{-}O_2CCO_2)]$ (prepared from 0.694 g, 1.97 mmol, of $W(CO)_6$ and 0.724 g, 2.08 mmol, of $[Et_4N]_2[C_2O_4]$) was added an additional 1 equiv of $W(CO)_5CH_3CN$ (0.693 g, 1.97 mmol, of $W(CO)_6$, photolyzed in CH_3CN for 30 min). Heating the bright orange solution at 50 °C for 36 h gave >50% conversion to the dimeric product: IR

(1) Darensbourg, D. J.; Rokicki, A.; Darensbourg, M. Y. *J. Am. Chem. Soc.* **1981**, *103*, 3223.
(2) Darensbourg, D. J.; Wiegreffe, H. P.; Wiegreffe, P. W. *J. Am. Chem. Soc.* **1990**, *112*, 9252.
(3) Bo, C.; Dedieu, A. *Inorg. Chem.* **1989**, *28*, 304.
(4) Darensbourg, D. J.; Joyce, J. A.; Bischoff, C. J.; Reibenspies, J. R. *Inorg. Chem.* **1991**, *30*, 1137.
(5) (a) Amatore, C.; Savéant, J. M. *J. Am. Chem. Soc.* **1981**, *103*, 5021. (b) Tezuka, M.; Yajima, T.; Tsuchija, A.; Matsumoto, Y.; Uchida, Y.; Hidai, M. *J. Am. Chem. Soc.* **1982**, *104*, 6834.

0020-1669/92/1331-3428$03.00/0

(CH_3CN) ν_{CO} 1997 (w), 1869 (s), 1839 (s), 1797 (m) cm^{-1}; IR (CH_3CN) ν_{COO^-} 1637 (s) cm^{-1}.

Synthesis of $[PPN]_2[W_2(CO)_{10}O_2CCO_2]$. A solution of $W(CO)_6$ (0.302 g, 0.858 mmol, in 40 mL of THF) was placed in a water-jacketed photolysis vessel, and a vigorous stream of nitrogen was bubbled through the solution. After 25 min of photolysis, the infrared spectrum of the solution indicated the major component to be $W(CO)_5THF$ with a trace of $W(CO)_6$ remaining. The orange photoproduct was transferred via cannula to a flask containing a slurry of $[PPN]_2[C_2O_4]$[6] (0.491 g, 0.422 mmol, in 10 mL of THF). The solution was stirred at room temperature for 1.5 h, after which the infrared spectrum in the ν_{CO} region showed a three-band pattern typical of an $M(CO)_5$ moiety containing an anionic ligand. Two additional bands were also present in the infrared spectrum, which were due to a small amount of the chelated complex. Pressurizing the solution with CO for 10 min resulted in a yellow solution, containing only the monodentate product. Concentration under reduced pressure followed by addition of ether and hexane afforded a yellow powder. The product was washed three times with 20-mL portions of hexane, dried briefly under reduced pressure, and purged for 15 min with CO gas: >75% yield; IR (THF) ν_{CO} 2063 (w), 1916 (s), 1857 (m) cm^{-1}. Anal. Calcd for $W_2C_{84}H_{60}O_{14}N_2P_4$: C, 55.6; H, 3.3. Found: C, 55.4; H, 3.5. Note: The product cannot be isolated completely free of $[PPN]_2[W_2(CO)_8(\eta^2\text{-}O_2CCO_2)]$, and drying under reduced pressure for extended periods of time results in extensive conversion to the chelated product.

Synthesis of $[PPN]_2[W_2(CO)_8(\eta^2\text{-}O_2CCO_2)]$. A THF solution of $[PPN]_2[W_2(CO)_{10}O_2CCO_2]$ was heated gently in a water bath (30–35 °C) with a stream of N_2 bubbling through the solution. Within 15 min, the η^2 species was observed by infrared spectroscopy. A total reaction time of 3 h resulted in an orange precipitate. The supernatant was removed, and the solid was washed three times with 10-mL portions of THF and dried under reduced pressure. The solid was readily soluble in acetonitrile. The reaction was quantitative by infrared spectroscopy: IR (CH_3CN) ν_{CO} 2001 (w), 1877 (s), 1844 (m), 1804 (m) cm^{-1}; IR (CH_3CN) ν_{COO^-} 1643 (s) cm^{-1}. X-ray-quality crystals were obtained by low-temperature crystallization from acetonitrile and diethyl ether. An infrared spectrum of the crystals in acetonitrile was identical to that of the bulk product.

Synthesis of $[PPN]_2[W_2(^{13}CO)_8(\eta^2\text{-}O_2CCO_2)]$. A solution of freshly sublimed $W(^{13}CO)_6$ (0.153 g, 0.427 mmol, in 20 mL of THF) was placed in a water-jacketed vessel with a vigorous stream of nitrogen bubbling through the solution. After 10 min of photolysis, the photoproduct was transferred via cannula to a flask containing a slurry of $[PPN]_2[C_2O_4]$ (0.467 g, 0.389 mmol, in 10 mL of THF). The orange solution was stirred at room temperature for 2 h. Infrared spectroscopy indicated a mixture of η^1 and η^2 products. The solution was swept with a vigorous stream of nitrogen, resulting in formation of an orange crystalline solid. The solid was washed with THF, dried, and dissolved in acetonitrile: ^{13}C NMR (CD_3CN) 218.1 (s), 205.3 (s) ppm. Infrared spectroscopy showed no shift in the strong ν_{COO^-} band relative to that of the unenriched species, indicating little coupling of this band to the ν_{CO} bands: IR (CH_3CN) ν_{CO} 1985 (w), 1871 (s), 1858 (s), 1833 (s), 1806 (m), 1775 (m), 1726 (w) cm^{-1}; IR (CH_3CN) ν_{COO^-} 1642 (vs) cm^{-1}.

X-ray Structural Determination of $[Et_4N]_2[1]$. A yellow irregularly shaped crystal was mounted on a glass fiber with vacuum grease at room temperature and cooled to 193 K in a N_2 cold stream. Preliminary examination and data collection were performed on a Nicolet R3m/V X-ray diffractometer (oriented graphite monochromator; Mo Kα radiation, λ = 0.710 73 Å).[7a] The diameter of the collimated X-ray beam was 1.0 mm. Cell parameters were calculated from the least-squares fitting of the setting angles for 22 reflections. ω scans for several intense reflections indicated acceptable crystal quality.

Data were collected for $4.0° \le 2\theta \le 50.0°$ at 193 K, with $-10 \le h \le 9$, $0 \le k \le 29$, and $0 \le l \le 15$. The scan range on ω for the data collection was 1.20° plus the Kα separation, with a variable scan rate of 2.00–15.00° min^{-1}. Three control reflections, collected every 97 reflections, showed no significant trends. A background measurement by the stationary-crystal/stationary-counter technique was taken at the beginning and end of each scan for half of the total scan time.

Lorentz and polarization corrections were applied to 4686 reflections. An empirical absorption correction was applied.[7b] A total of 2890 unique reflections with $F > 4.0\sigma(F)$ were used in further calculations. The structure was solved by a Patterson synthesis.[7c] Full-matrix least-squares anisotropic refinement for all non-hydrogen atoms[7d] yielded $R = 0.055$, $R_w = 0.047$, and $S = 1.38$ at convergence. Hydrogen atoms were placed in idealized positions with isotropic thermal parameters fixed at 0.08 Å^2. Neutral-atom scattering factors and anomalous scattering correction terms were taken from a standard source.[7e] Crystal data and experimental conditions are provided in Table I.

Table I. Crystallographic Data and Data Collection Parameters

	$[EtN_4]_2[1]$	$[PPN]_2[2]\cdot^1/_2(CH_3CH_2)_2O$
formula	$C_{22}H_{40}N_2O_8W$	$C_{43}H_{35}NO_{6.5000}P_2W$
fw	644.4	915.5
space group	monoclinic, $P2_1/n$ (No. 14)	monoclinic, $P2_1/c$ (No. 14)
a, Å	8.581 (5)	14.745 (7)
b, Å	24.773 (9)	12.916 (4)
c, Å	13.151 (5)	20.415 (9)
β, deg	108.56 (3)	95.60 (4)
V, Å^3	2650 (2)	3869 (3)
Z	4	2
d(calcd), g/cm^3	1.615	1.572
abs coeff, mm^{-1}	4.495	3.178
λ, Å	0.710 73	0.710 73
T, K	193	193
transm coeff	0.4984–0.8429	0.8094–0.9903
R,[a] %	5.51	6.47
R_w,[a] %	4.70	6.08

[a] $R = \sum|F_o - F_c|/\sum F_o$. $R_w = \{[\sum w(F_o - F_c)^2]/[\sum w(F_o)^2]\}^{1/2}$. GOF = 1.38 and 2.55 for $[EtN_4]_2[1]$ and $[PPN]_2[2]\cdot^1/_2(CH_3CH_2)_2O$, respectively.

X-ray Structural Determination of $[PPN]_2[2]\cdot^1/_2(CH_3CH_2)_2O$. A yellow plate was mounted on a glass fiber with vacuum grease at room temperature and cooled to 193 K in a N_2 cold stream. Preliminary examination and data collection were performed on the same Nicolet R3m/V X-ray diffractometer. The diameter of the collimated X-ray beam was 0.5 mm. Cell parameters were calculated from the least-squares fitting of the setting angles of 25 reflections. ω scans for several intense reflections indicated acceptable crystal quality.

Data were collected for $4.0° \le 2\theta \le 50.0°$ at 193 K, with $-17 \le h \le 17$, $-15 \le k \le 3$, and $-24 \le l \le 24$. The scan range for the data collection was 0.60° plus the Kα separation, with a variable scan rate of 1.50–14.65° min^{-1}. Three control reflections, collected every 97 reflections, showed no significant trends. A background measurement by the stationary-crystal/stationary-counter technique was done at the beginning and end of each scan for half of the total scan time.

Lorentz and polarization corrections were applied to 7317 reflections. A semiempirical[7f] absorption correction was applied (T_{max} = 0.9903, T_{min} = 0.8094). A total of 4695 unique reflections (R_{int} = 0.04) with $F > 4.0\sigma(F)$ were used in further calculations. The structure was solved by a Patterson synthesis.[7c] Full-matrix least-squares isotropic refinement for O(1ET) and C(1ET) and anisotropic refinement for all remaining non-hydrogen atoms yielded $R = 0.065$, $R_w = 0.061$, and $S = 2.55$ at convergence. The extinction coefficient was refined to 0.001 14 (2).[7g] Hydrogen atoms were placed in idealized positions with isotropic thermal parameters fixed at 0.08 Å^2. Neutral-atom scattering factors and anomalous scattering correction terms were taken from a standard source.[7e] Atomic distances were constrained as follows. The distance between atoms in the pair (O(1ET), C(1ET)) was constrained to 1.40 (±0.01) Å, and the distance between the atoms in the pair (C(2ET), C(1ET)) was constrained to 1.54 (±0.01) Å. Atom O(1ET) was found to only partially fill its site in the asymmetric unit of the crystallographic unit cell, and its site occupation was fixed to 50%. The constrained model, corrected for variable site occupation, was used to refine the structure to convergence.

(6) Martiusen, A.; Songstad, J. *Acta Chem. Scand., Ser. A* **1977**, *A31*, 645.

(7) (a) Control software, P3VAX (3.42), was supplied by Nicolet Analytical X-ray Instruments, Madison, WI. (b) Straut, D.; Walker, N. *Acta Crystallogr.* **1983**, *A39*, 158. (c) All crystallographic calculations were performed on a μVaxII minicomputer with SHELXTL-PLUS, revision 3.4 (G. M. Sheldrick, Institüt für Anorganische Chemie der Universität, Tammannstrasse 4, D-3400 Gottingen, Germany), supplied by Nicolet Analytical X-ray Instruments, Madison, WI. (d) Number of least-squares parameters 298; quantity minimized $\sum w(F_o - F_c)^2$; $w^{-1} = \sigma^2(F) + gF^2$, g = 0.000 10. (e) *International Tables for X-Ray Crystallography*; Ibers, J. A., Hamilton, W. S., Eds.; Kynoch Press: Birmingham, England, 1974; Vol. IV, pp 99, 149. (f) Several reflections were measured at intervals of ψ (the azimuthal angle corresponding to 360 rotations of the crystal about its diffraction vector). These reflections were then utilized to apply a semiempirical absorption correction to the remaining reflections. Program PSICOR: J. M. Williams and M. Beno, Argonne National Laboratory, July 1984. (g) Larson, A. C. *Acta Crystallogr.* **1967**, *A23*, 604.

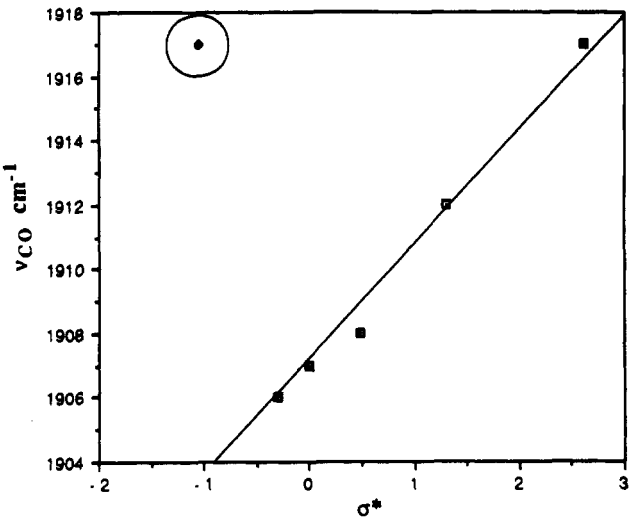

Figure 1. Infrared comparison for ν_{CO} (strong band, E mode) in $W(CO)_5O_2CR^-$ complexes (data taken from ref 4; ◆ = observed frequency for complex 3).

Diethyl ether and acetonitrile were the two possible solvent molecules accessible for inclusion in the compound $[PPN]_2[2]$. The solvent molecule sits about the inversion center; thus if acetonitrile were the solvent, it would have to be disordered (only 50% occupation). Acetonitrile was ruled out because of the high electron density associated with each solvent atom. The electron density seen for each solvent atom is much greater than the disordered model would predict. The bond lengths (1.408 and 1.519 Å) are also not consistent with an acetonitrile molecule, although the central bond angle (171°) is consistent with this solvent species. Diethyl ether, on the other hand, is consistent with the observed electron density and the bond length. The deviation in the bond angle may be a product of the large thermal displacement parameters and may indicate possible disorder in the terminal carbon atom of the solvent. Crystal data and experimental conditions are provided in Table I.

Results

Synthesis and Reactivity of $W(CO)_4(\eta^2\text{-}O_2CCO_2)^{2-}$ and $W_2(CO)_8(\eta^2\text{-}O_2CCO_2)^{2-}$. The monomeric complex $W(CO)_4(\eta^2\text{-}O_2CCO_2)^{2-}$ was prepared by the addition of 1 equiv of $[Et_4N]_2[O_2CCO_2]$ to $W(CO)_5CH_3CN$ in acetonitrile. As expected for a carboxylate containing a good donor group (i.e. R = CO_2^-, $\sigma^* = -1.06$, eq 1),[4] the η^2 species forms spontaneously from the initially afforded η^1 species upon heating. The complex reacts slowly, however, with an additional 1 equiv of $W(CO)_5CH_3CN$ to form the dimeric species $W_2(CO)_8(\eta^2\text{-}O_2CCO_2)^{2-}$.

Alternatively, the dimeric species $[PPN]_2[W_2(CO)_8(\eta^2\text{-}O_2CCO_2)]$ can be prepared by the addition of $[PPN]_2[C_2O_4]$ to an excess of $W(CO)_5THF$ in THF solution. The η^1 dimeric complex, $W_2(CO)_{10}(O_2CCO_2)^{2-}$, is the first complex formed. The infrared frequencies observed for this derivative at 1917 cm^{-1} (strong band) and 1850 cm^{-1} (medium band) are significantly higher than what is predicted for the monomeric product, $W(CO)_5(\eta^1\text{-}C_2O_4)^{2-}$. That is, the values for the monomeric η^1 complex, predicted from a plot of σ^* versus ν_{CO} for several known tungsten carboxylates[4] (see Figure 1) are 1903 cm^{-1} (strong band) and 1836 cm^{-1} (medium band). The η^2 complex, $W_2(CO)_8(\eta^2\text{-}O_2CCO_2)^{2-}$, was formed by sweeping the solution with a stream of nitrogen gas at ambient temperature. Formation of the dimeric species is favored in THF solution due to the limited solubility of $[PPN]_2[C_2O_4]$ in this solvent.

Solid-State Structure of $[Et_4N]_2[1]$. The structure of $[Et_4N]_2[W(CO)_4(\eta^2\text{-}O_2CCO_2)]$ was defined by single-crystal X-ray diffraction. Suitable crystals were isolated from acetonitrile and diethyl ether. The crystal was mounted in open air at room temperature and immediately cooled to 193 K. Final atomic coordinates for all non-hydrogen atoms are given in Table II. A view of the dianion is shown in Figure 2, and selected bond lengths and angles are listed in Tables III and IV.

Table II. Atomic Coordinates (×10^4) and Equivalent Isotropic Displacement Parameters (Å^2 × 10^3) for $C_{22}H_{40}N_2O_8W$[a]

	x	y	z	U(eq)[b]
W(1)	128 (1)	1191 (1)	3974 (1)	22 (1)
C(1)	−251 (14)	1973 (6)	3870 (10)	27 (5)
O(1)	−314 (12)	2448 (4)	3987 (8)	50 (5)
C(2)	1049 (15)	435 (6)	4471 (9)	25 (5)
O(2)	1802 (11)	69 (4)	4891 (7)	38 (4)
C(3)	2184 (16)	1434 (6)	4981 (10)	28 (5)
O(3)	3413 (10)	1593 (4)	5620 (7)	41 (4)
C(4)	−834 (14)	1179 (6)	5137 (9)	26 (4)
O(4)	−1427 (11)	1184 (5)	5816 (6)	44 (4)
C(5)	−296 (16)	947 (6)	1632 (9)	27 (5)
C(6)	−1999 (15)	842 (6)	1758 (10)	30 (5)
O(5)	−23 (11)	874 (4)	794 (6)	32 (4)
O(6)	−3123 (10)	682 (4)	980 (6)	36 (4)
O(7)	828 (9)	1116 (4)	2523 (6)	29 (3)
O(8)	−2116 (10)	929 (4)	2705 (6)	28 (3)
N(1)	−3709 (12)	546 (4)	−2164 (7)	22 (4)
C(9)	−609 (15)	391 (6)	−1718 (10)	34 (5)
C(10)	−2126 (14)	294 (5)	−1426 (9)	25 (5)
C(11)	−3522 (15)	1152 (6)	−2257 (9)	34 (5)
C(12)	−2947 (16)	1454 (6)	−1216 (10)	42 (6)
C(13)	−6746 (16)	616 (7)	−2282 (11)	46 (7)
C(14)	−5051 (17)	418 (6)	−1650 (10)	38 (6)
C(15)	−4145 (15)	309 (5)	−3277 (8)	26 (5)
C(16)	−4472 (16)	−292 (6)	−3387 (9)	32 (6)
N(2)	4016 (12)	2028 (5)	1815 (7)	29 (4)
C(17)	928 (16)	2257 (6)	1140 (11)	46 (6)
C(18)	2670 (17)	2423 (6)	1196 (11)	46 (6)
C(19)	3999 (16)	2019 (6)	2951 (9)	32 (5)
C(20)	5471 (16)	1730 (5)	3762 (9)	33 (6)
C(21)	5656 (16)	2237 (7)	1739 (11)	44 (6)
C(22)	6174 (19)	2787 (7)	2238 (13)	63 (8)
C(23)	3319 (16)	1407 (7)	183 (9)	52 (7)
C(24)	3698 (16)	1465 (6)	1372 (9)	39 (6)

[a] Estimated standard deviations are given in parentheses. [b] Equivalent isotropic U defined as one-third of the trace of the orthogonalized U_{ij} tensor.

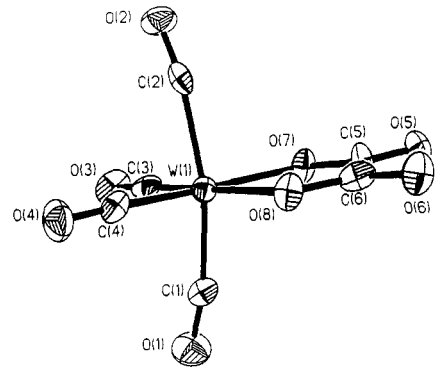

Figure 2. Thermal ellipsoid plot (50% probability) of **1**.

The complex exists as a distorted octahedron. The average W–C bond distance for the axial carbonyl ligands is 2.01 Å, whereas the analogous distance for the equatorial carbonyl ligands is 1.95 Å. The axial carbonyl ligands are bent away from the oxalate ligand, forming a C(2)–W(1)–C(1) angle of 163.7°. The equatorial carbonyls, however, are unaffected by the oxalate ligand, having a C(3)–W–C(4) angle of 89.4°. The bite angle of the oxalate ligand with the metal center is small, at 74.4°, but significantly larger than that of 59.5° seen in the tungsten carbonate species.[8] The C–C bond of the oxalate ligand shows little double character at 1.54 Å.

Solid-State Structure of $[PPN]_2[2]\cdot{}^1/_2(CH_3CH_2)_2O$. Single-crystal X-ray diffraction was employed to define the molecular structure of $[PPN]_2[W_2(CO)_8(\eta^2\text{-}O_2CCO_2)]$. Yellow crystals

(8) Darensbourg, D. J.; Sanchez, K. M.; Rheingold, A. L. *J. Am. Chem. Soc.* **1987**, *109*, 290.

Table III. Bond Lengths (Å) for $C_{22}H_{40}N_2O_8W$[a]

W(1)–C(1)	1.96 (1)	W(1)–C(2)	2.06 (1)
W(1)–C(3)	1.93 (1)	W(1)–C(4)	1.96 (1)
W(1)–O(7)	2.184 (8)	W(1)–O(8)	2.207 (7)
C(1)–O(1)	1.19 (2)	C(2)–O(2)	1.15 (2)
C(3)–O(3)	1.19 (1)	C(4)–O(4)	1.16 (2)
C(5)–C(6)	1.54 (2)	C(5)–O(5)	1.21 (2)
C(5)–O(7)	1.33 (1)	C(6)–O(6)	1.23 (1)
C(6)–O(8)	1.30 (2)	N(1)–C(10)	1.53 (1)
N(1)–C(11)	1.52 (2)	N(1)–C(14)	1.54 (2)
N(1)–C(15)	1.51 (1)	C(9)–C(10)	1.49 (2)
C(11)–C(12)	1.50 (2)	C(13)–C(14)	1.51 (2)
C(15)–C(16)	1.51 (2)	N(2)–C(18)	1.53 (2)
N(2)–C(19)	1.50 (2)	N(2)–C(21)	1.53 (2)
N(2)–C(24)	1.50 (2)	C(17)–C(18)	1.53 (2)
C(19)–C(20)	1.54 (2)	C(21)–C(22)	1.52 (2)
C(23)–C(24)	1.50 (2)		

[a] Estimated standard deviations are given in parentheses.

Table IV. Bond angles (deg) for $C_{22}H_{40}N_2O_8W$[a]

C(1)–W(1)–C(2)	163.7 (4)	C(1)–W(1)–C(3)	80.5 (5)
C(2)–W(1)–C(3)	83.8 (5)	C(1)–W(1)–C(4)	88.2 (6)
C(2)–W(1)–C(4)	87.3 (6)	C(3)–W(1)–C(4)	89.4 (5)
C(1)–W(1)–O(7)	96.2 (5)	C(2)–W(1)–O(7)	90.9 (5)
C(3)–W(1)–O(7)	100.4 (5)	C(4)–W(1)–O(7)	169.8 (4)
C(1)–W(1)–O(8)	98.8 (4)	C(2)–W(1)–O(8)	97.3 (4)
C(3)–W(1)–O(8)	174.6 (5)	C(4)–W(1)–O(8)	95.9 (4)
O(7)–W(1)–O(8)	74.4 (3)	W(1)–C(1)–O(1)	169 (1)
W(1)–C(2)–O(2)	167 (1)	W(1)–C(3)–O(3)	177 (1)
W(1)–C(4)–O(4)	178 (1)	C(6)–C(5)–O(5)	122 (1)
C(6)–C(5)–O(7)	114 (1)	O(5)–C(5)–O(7)	124 (1)
C(5)–C(6)–O(6)	119 (1)	C(5)–C(6)–O(8)	116 (1)
O(6)–C(6)–O(8)	125 (1)	W(1)–O(7)–C(5)	118.3 (8)
W(1)–O(8)–C(6)	117.3 (8)	C(10)–N(1)–C(11)	111.1 (8)
C(10)–N(1)–C(14)	105.9 (9)	C(11)–N(1)–C(14)	111 (1)
C(10)–N(1)–C(15)	110.7 (9)	C(11)–N(1)–C(15)	107.8 (9)
C(14)–N(1)–C(15)	110.8 (9)	N(1)–C(10)–C(9)	116 (1)
N(1)–C(11)–C(12)	116 (1)	N(1)–C(14)–C(13)	115 (1)
N(1)–C(15)–C(16)	117 (1)	C(18)–N(2)–C(19)	107 (1)
C(18)–N(2)–C(21)	108 (1)	C(19)–N(2)–C(21)	111.8 (9)
C(18)–N(2)–C(24)	111.9 (9)	C(19)–N(2)–C(24)	108 (1)
C(21)–N(2)–C(24)	110 (1)	N(2)–C(18)–C(17)	114 (1)
N(2)–C(19)–C(20)	115 (1)	N(2)–C(21)–C(22)	115 (1)
N(2)–C(24)–C(23)	117 (1)		

[a] Estimated standard deviations are given in parentheses.

suitable for X-ray analysis were isolated from acetonitrile/diethyl ether. The crystal was mounted in open air at room temperature and immediately cooled to 193 K. Final atomic coordinates for all non-hydrogen atoms are given in Table V. A view of the dianion is shown in Figure 3. Selected bond lengths and bond angles for the complex are listed in Tables VI and VII.

The dimeric dianion lies on a center of symmetry, with the arrangement of ligands about each tungsten center found to be that of a distorted octahedron. The average W–C bond distance for the axial carbonyl ligands is 2.021 Å, while that for the equatorial ligands is 1.957 Å. The four CO ligands bend away from the bridging oxalate ligand such that the axial carbonyl carbon atoms form an angle with the tungsten atom (C(1)–W(1)–C(2)) of 170.7° and the equatorial carbonyl atoms are compressed to an angle (C(1)–W(1)–C(2)) of 85.9°. The bite angle of the oxalate ligand with the metal center (O(5)–W(1)–O(6a)) is 72.7°; this value is significantly larger than the angle found for the monomeric tungsten carbonate species,[8] but slightly smaller than the analogous angle found in other dimeric oxalate complexes.[9] The oxalate ligand is planar, with a C–C bond distance of 1.538 Å, typical for similar species.[9,10]

Table V. Atomic Coordinates (×10⁴) and Equivalent Isotropic Displacement Parameters (Å² × 10³) for $C_{43}H_{35}NO_{6.5000}P_2W$[a]

	x	y	z	U(eq)[b]
W(1)	3928 (1)	282 (1)	1123 (1)	35 (1)
O(5)	5346 (5)	426 (7)	796 (3)	43 (3)
O(6)	6138 (5)	282 (7)	−79 (3)	44 (3)
C(5)	5430 (7)	200 (9)	205 (5)	34 (4)
C(1)	2645 (8)	117 (8)	1313 (5)	35 (4)
O(1)	1915 (6)	13 (6)	1434 (4)	54 (4)
C(2)	4151 (8)	779 (9)	2018 (6)	40 (4)
O(2)	4273 (6)	1075 (6)	2565 (4)	55 (3)
C(3)	3591 (11)	1743 (14)	830 (6)	69 (7)
O(3)	3323 (8)	2587 (8)	703 (5)	83 (5)
C(4)	4072 (7)	−1166 (14)	1485 (6)	54 (6)
O(4)	4073 (7)	−1992 (8)	1750 (5)	72 (4)
P(1)	8047 (2)	900 (2)	2221 (1)	24 (1)
P(2)	9190 (2)	722 (2)	3516 (1)	26 (1)
N	8838 (6)	1039 (7)	2793 (4)	31 (3)
C(6)	8008 (8)	3031 (9)	2205 (6)	41 (4)
C(7)	7600 (11)	3980 (11)	2053 (6)	60 (6)
C(8)	6743 (11)	4030 (10)	1717 (7)	57 (6)
C(9)	6276 (9)	3151 (11)	1512 (6)	53 (5)
C(10)	6651 (8)	2177 (10)	1666 (5)	43 (5)
C(11)	7533 (8)	2130 (8)	2006 (5)	32 (4)
C(12)	6998 (8)	−887 (9)	2086 (6)	44 (5)
C(13)	6352 (8)	−1567 (10)	2279 (6)	45 (5)
C(14)	5847 (8)	−1340 (9)	2794 (6)	46 (5)
C(15)	5967 (7)	−374 (10)	3108 (6)	47 (5)
C(16)	6626 (7)	325 (9)	2918 (5)	36 (4)
C(17)	7128 (6)	58 (7)	2409 (5)	24 (4)
C(18)	9356 (7)	−175 (9)	1617 (5)	35 (4)
C(19)	9720 (9)	−677 (9)	1114 (6)	49 (5)
C(20)	9252 (9)	−636 (8)	491 (6)	43 (5)
C(21)	8429 (10)	−133 (10)	389 (5)	51 (5)
C(22)	8060 (8)	377 (9)	901 (5)	37 (4)
C(23)	8530 (6)	338 (8)	1524 (4)	23 (3)
C(24)	10156 (8)	−1115 (9)	3808 (6)	40 (4)
C(25)	10266 (9)	−2180 (10)	3891 (7)	53 (5)
C(26)	9479 (9)	−2785 (10)	3778 (6)	45 (5)
C(27)	8650 (8)	−2355 (9)	3606 (6)	45 (5)
C(28)	8563 (9)	−1300 (9)	3539 (6)	43 (5)
C(29)	9307 (7)	−633 (8)	3631 (5)	25 (4)
C(30)	10835 (8)	1476 (8)	3183 (5)	38 (4)
C(31)	11739 (8)	1831 (9)	3322 (7)	50 (5)
C(32)	12062 (8)	2037 (10)	3960 (6)	48 (5)
C(33)	11547 (9)	1870 (9)	4469 (6)	46 (5)
C(34)	10657 (7)	1496 (8)	4337 (5)	30 (4)
C(35)	10294 (8)	1284 (8)	3696 (5)	30 (4)
C(36)	8231 (7)	587 (9)	4626 (5)	39 (4)
C(37)	7674 (9)	992 (11)	5074 (6)	53 (5)
C(38)	7406 (8)	2008 (11)	5023 (6)	51 (5)
C(39)	7650 (8)	2626 (9)	4525 (6)	44 (5)
C(40)	8185 (7)	2228 (9)	4063 (5)	36 (4)
C(41)	8482 (7)	1192 (8)	4116 (5)	29 (4)
O(1ET)	4917 (19)	−318 (20)	4853 (13)	118 (10)
C(1ET)	4779 (20)	725 (23)	4669 (14)	197 (12)
C(2ET)	4784 (21)	1875 (21)	4512 (15)	214 (13)

[a] Estimated standard deviations are given in parentheses. [b] Equivalent isotropic U defined as one-third of the trace of the orthogonalized U_{ij} tensor.

Discussion

The reactions involving displacement of labile solvent molecules (THF or CH_3CN) by the oxalate anion observed herein are summarized in Scheme I. As previously mentioned, studies from our laboratories have shown that the rate of cis CO substitution in $(CO)_5MO_2CR^-$ complexes is enhanced by electron-releasing R substituents on the monodentate carboxylate ligand.[4] Hence, the anticipated first-formed product from the reaction of $W(CO)_5CH_3CN$ with excess $[Et_4N]_2[C_2O_4]$, species **4**, would be predicted to lose a CO ligand with a rate constant of 3.0×10^{-2}

(9) Felthouse, T. R.; Laskowski, E. J.; Hendrickson, D. N. *Inorg. Chem.* **1977**, *16*, 1077.
(10) Bottomley, F.; Lin, E. J. B.; White, P. S. *J. Organomet. Chem.* **1981**, *212*, 341.
(11) Darensbourg, D. J.; Sanchez, K. M.; Reibenspies, J. H.; Rheingold, A. L. *J. Am. Chem. Soc.* **1989**, *111*, 7094.
(12) For a preliminary report of this structure, see: Mueller, B. L.; Darensbourg, D. J. *Proceedings of the International Symposium on Chemical Fixation of Carbon Dioxide*, Nagoya, Japan; The Chemical Society of Japan: Nagoya, Japan, 1991; abstract B19.

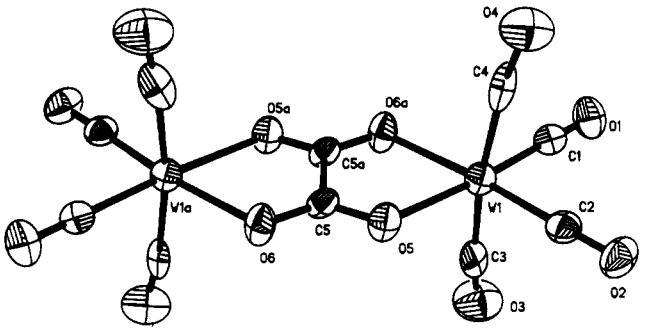

Figure 3. Thermal ellipsoid plot (50% probability) of **2**.

Table VI. Bond Lengths (Å) for $C_{43}H_{35}NO_{6.5000}P_2W$[a]

W(1)–O(5)	2.263 (7)	W(1)–C(1)	1.979 (12)
W(1)–C(2)	1.934 (12)	W(1)–C(3)	2.026 (18)
W(1)–C(4)	2.015 (17)	W(1)–O(6a)	2.245 (7)
O(5)–C(5)	1.260 (13)	O(6)–C(5)	1.248 (13)
O(6)–W(1a)	2.245 (7)	C(5)–C(5a)	1.538 (20)
C(1)–O(1)	1.136 (15)	C(2)–O(2)	1.178 (14)
C(3)–O(3)	1.180 (21)	C(4)–O(4)	1.196 (20)
P(1)–N	1.578 (8)	P(1)–C(11)	1.795 (11)
P(1)–C(17)	1.808 (10)	P(1)–C(23)	1.806 (10)
P(2)–N	1.570 (8)	P(2)–C(29)	1.772 (11)
P(2)–C(35)	1.787 (11)	P(2)–C(41)	1.792 (11)
C(6)–C(7)	1.387 (18)	C(6)–C(11)	1.399 (16)
C(7)–C(8)	1.379 (21)	C(8)–C(9)	1.372 (20)
C(9)–C(10)	1.396 (19)	C(10)–C(11)	1.415 (15)
C(12)–C(13)	1.381 (17)	C(12)–C(17)	1.391 (15)
C(13)–C(14)	1.379 (18)	C(14)–C(15)	1.406 (18)
C(15)–C(16)	1.408 (17)	C(16)–C(17)	1.377 (15)
C(18)–C(19)	1.367 (17)	C(18)–C(23)	1.383 (14)
C(19)–C(20)	1.388 (18)	C(20)–C(21)	1.374 (19)
C(21)–C(22)	1.392 (16)	C(22)–C(23)	1.387 (13)
C(24)–C(25)	1.394 (17)	C(24)–C(29)	1.413 (16)
C(25)–C(26)	1.399 (18)	C(26)–C(27)	1.357 (17)
C(27)–C(28)	1.374 (16)	C(28)–C(29)	1.393 (16)
C(30)–C(31)	1.412 (16)	C(30)–C(35)	1.400 (16)
C(31)–C(32)	1.369 (18)	C(32)–C(33)	1.362 (18)
C(33)–C(34)	1.399 (16)	C(34)–C(35)	1.392 (14)
C(36)–C(37)	1.391 (17)	C(36)–C(41)	1.381 (15)
C(37)–C(38)	1.371 (19)	C(38)–C(39)	1.368 (18)
C(39)–C(40)	1.387 (16)	C(40)–C(41)	1.409 (15)
O(1ET)–C(1ET)	1.408 (39)	O(1ET)–O(1EA)	1.034 (51)
O(1ET)–C(1EA)	1.160 (38)	C(1ET)–C(2ET)	1.519 (41)
C(1ET)–O(1EA)	1.160 (38)		

[a] Estimated standard deviations are given in parentheses.

s^{-1} at 40 °C.[13] That is, the half-life of species **4** with respect to formation of **1** would be about 23 s at 40 °C, or complete formation of **1** would be expected to occur within a few minutes. Indeed, the anticipated intermediate, **4**, was not observed during the synthesis of **1**. Furthermore, because of the rapid ring-opening process observed for other chelated $W(CO)_4(\eta^2\text{-}O_2CR)^-$ derivatives,[14] it is expected that **4** could proceed to the thermodynamic product **1** via the intermediacy of **5** (Scheme II).

By way of contrast, upon reaction of the oxalate anion with 2 equiv of $W(CO)_5THF$, $[(CO)_5W]_2C_2O_4^{2-}$ is observed and found to be a stable complex. However, during solvent removal, some loss of CO occurs, leading to formation of species **2**. Hence, it was not possible to isolate $[(CO)_5W]_2C_2O_4^{2-}$ totally in the absence of the chelated derivative **2**. Metalation of the $-CO_2^-$ substituent in **4**, i.e., formation of **3**, greatly stabilizes the $-W(CO)_5$ unit toward CO dissociation. On the basis of the ν_{CO} correlation with σ^* (Figure 1), a σ^* value of +2.6 for the $-CO_2W(CO)_5^-$ substituent is predicted. This value indicates that metalation of the CO_2^- moiety to produce $-CO_2W(CO)_5^-$ results in a somewhat more electron-withdrawing substituent than protonation or alkylation at the oxygen atom, e.g., $-CO_2R$ (R = H or Et, σ^* = 2.08 or 2.12, respectively). Concomitantly, the rate constant anticipated for CO dissociation in **3** is about 1.0×10^{-4} s^{-1} at 40 °C or $t_{1/2}$ = 2 h,[13] consistent with the observed rate of formation of **2** from **3**.

(13) This value is determined from a plot of σ^* versus log k_{obs} at 40 °C. See ref 4.

(14) Darensbourg, D. J.; Wiegreffe, H. P. *Inorg. Chem.* **1990**, *29*, 592.

Table VII. Bond Angles (deg) for $C_{43}H_{35}NO_{6.5000}P_2W$[a]

O(5)–W(1)–C(1)	174.1 (4)	O(5)–W(1)–C(2)	100.0 (4)
C(1)–W(1)–C(2)	85.9 (5)	O(5)–W(1)–C(3)	92.5 (5)
C(1)–W(1)–C(3)	87.0 (5)	C(2)–W(1)–C(3)	89.1 (5)
O(5)–W(1)–C(4)	96.7 (4)	C(1)–W(1)–C(4)	84.1 (4)
C(2)–W(1)–C(4)	87.7 (5)	C(3)–W(1)–C(4)	170.7 (5)
O(5)–W(1)–O(6a)	72.7 (3)	C(1)–W(1)–O(6a)	101.4 (4)
C(2)–W(1)–O(6a)	172.7 (4)	C(3)–W(1)–O(6a)	92.0 (4)
C(4)–W(1)–O(6a)	92.3 (4)	W(1)–O(5)–C(5)	116.3 (6)
C(5)–O(6)–W(1a)	117.0 (6)	O(5)–C(5)–O(6)	126.2 (9)
O(5)–C(5)–C(5a)	116.5 (12)	O(6)–C(5)–C(5a)	117.2 (12)
W(1)–C(1)–O(1)	178.6 (9)	W(1)–C(2)–O(2)	178.8 (9)
W(1)–C(3)–O(3)	172.9 (13)	W(1)–C(4)–O(4)	171.6 (11)
N–P(1)–C(11)	110.2 (5)	N–P(1)–C(17)	115.3 (4)
C(11)–P(1)–C(17)	106.1 (5)	N–P(1)–C(23)	108.0 (4)
C(11)–P(1)–C(23)	110.6 (5)	C(17)–P(1)–C(23)	106.6 (5)
N–P(2)–C(29)	113.7 (5)	N–P(2)–C(35)	107.4 (5)
C(29)–P(2)–C(35)	107.4 (5)	N–P(2)–C(41)	113.1 (5)
C(29)–P(2)–C(41)	107.4 (5)	C(35)–P(2)–C(41)	107.6 (5)
P(1)–N–P(2)	145.0 (6)	C(7)–C(6)–C(11)	118.5 (11)
C(6)–C(7)–C(8)	120.6 (13)	C(7)–C(8)–C(9)	121.3 (13)
C(8)–C(9)–C(10)	120.1 (12)	C(9)–C(10)–C(11)	118.3 (11)
P(1)–C(11)–C(6)	118.5 (8)	P(1)–C(11)–C(10)	120.3 (9)
C(6)–C(11)–C(10)	121.1 (10)	C(13)–C(12)–C(17)	119.3 (11)
C(12)–C(13)–C(14)	121.4 (11)	C(13)–C(14)–C(15)	118.8 (11)
C(14)–C(15)–C(16)	120.2 (11)	C(15)–C(16)–C(17)	118.9 (10)
P(1)–C(17)–C(12)	119.9 (8)	P(1)–C(17)–C(16)	118.5 (8)
C(12)–C(17)–C(16)	121.2 (10)	C(19)–C(18)–C(23)	121.9 (10)
C(18)–C(19)–C(20)	118.3 (11)	C(19)–C(20)–C(21)	120.6 (12)
C(20)–C(21)–C(22)	120.9 (11)	C(21)–C(22)–C(23)	118.3 (10)
P(1)–C(23)–C(18)	119.6 (7)	P(1)–C(23)–C(22)	120.5 (8)
C(18)–C(23)–C(22)	119.9 (9)	C(25)–C(24)–C(29)	123.7 (11)
C(24)–C(25)–C(26)	116.5 (11)	C(25)–C(26)–C(27)	121.7 (12)
C(26)–C(27)–C(28)	120.3 (11)	C(27)–C(28)–C(29)	122.4 (11)
P(2)–C(29)–C(24)	122.7 (8)	P(2)–C(29)–C(28)	121.9 (8)
C(24)–C(29)–C(28)	115.4 (10)	C(31)–C(30)–C(35)	120.2 (10)
C(30)–C(31)–C(32)	119.2 (12)	C(31)–C(32)–C(33)	121.8 (11)
C(32)–C(33)–C(34)	119.4 (11)	C(33)–C(34)–C(35)	121.0 (10)
P(2)–C(35)–C(30)	119.4 (8)	P(2)–C(35)–C(34)	122.2 (8)
C(30)–C(35)–C(34)	118.3 (10)	C(37)–C(36)–C(41)	120.1 (11)
C(36)–C(37)–C(38)	119.7 (12)	C(37)–C(38)–C(39)	121.3 (12)
C(38)–C(39)–C(40)	119.9 (11)	C(39)–C(40)–C(41)	119.5 (10)
P(2)–C(41)–C(36)	122.7 (8)	P(2)–C(41)–C(40)	117.8 (8)
C(36)–C(41)–C(40)	119.4 (10)	C(1ET)–O(1ET)–O(1EA)	54.1 (25)
C(1ET)–O(1ET)–C(1EA)	133.8 (24)	O(1EA)–O(1ET)–C(1EA)	79.6 (31)
O(1ET)–C(1ET)–C(2ET)	171.1 (28)	O(1ET)–C(1ET)–O(1EA)	46.2 (24)
C(2ET)–C(1ET)–O(1EA)	127.7 (28)		

[a] Estimated standard deviations are given in parentheses.

Scheme I

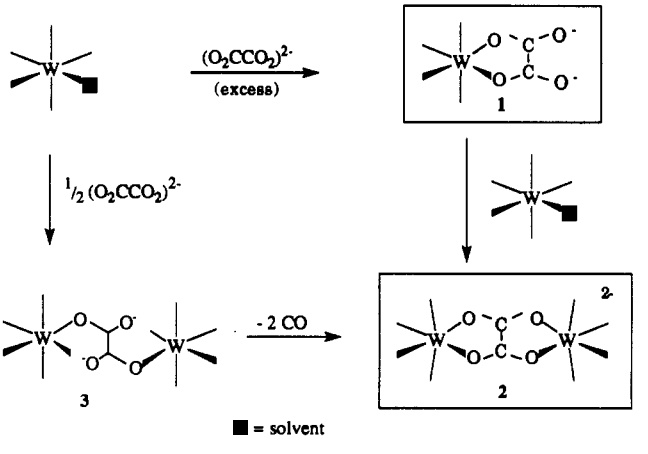

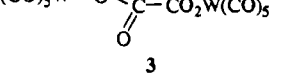

3

Comparative bond distances in the oxalate ligand, bonded as a bidentate and tetradentate ligand, are illustrated in Figure 4.

Table VIII. Comparative Structural and Spectral Data for Various Tungsten Complexes

complex	av M–CO, Å		OC–M–CO, deg		ν_{CO}, cm^{-1} (CH_3CN)	^{13}C NMR, ppm (CD_3CN)
	ax	eq	ax	eq		
$W(CO)_4C_2O_4^{2-}$	2.01	1.95	163.7	89.4	1986, 1847, 1825, 1782	205.4, 218.2
$W(CO)_4CO_3^{2-}$ [a]	2.016	1.935	165.7	87.9	1977, 1839, 1820, 1784	207.7, 215.6
$W(CO)_4(C_6H_4O_2)^{2-}$ [b]	1.965	1.909	167.3	87.5	1965, 1817, 1800, 1763	208.8, 219.6[c]

[a] Data taken from ref 11. [b] Data taken from ref 12. [c] At −30 °C.

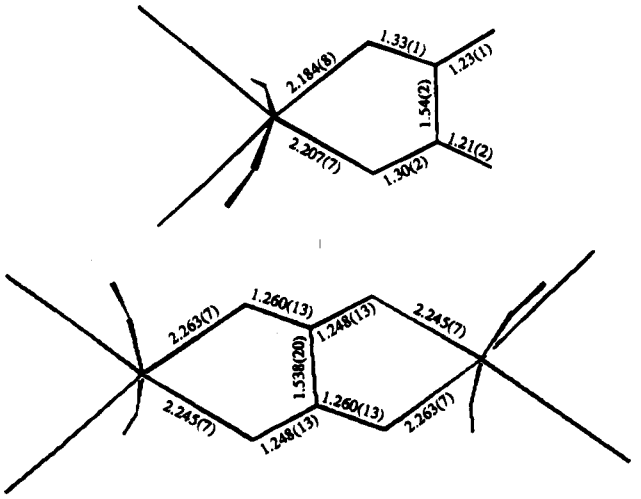

Figure 4. Comparative bond lengths for **1** and **2**.

Scheme II

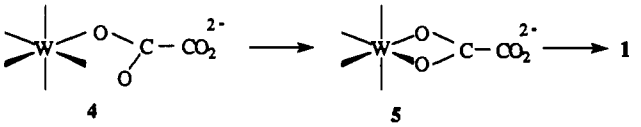

4 **5**

In the case of species **1**, in which the oxalate anion is chelated to one metal center by way of the two carboxylate groups, there are two long and two short C–O bond distances. The two distal oxygen atoms have the shorter C–O bond lengths. When all four oxygen atoms of $C_2O_4^{2-}$ are bound to two metal centers (species **2**), the C–O bond lengths are intermediate between the two short and two long C–O bond lengths of species **1**. Furthermore, the W–O bond lengths are longer in the dimeric complex **2** as compared to the corresponding bond lengths in the monomeric complex **1**. The only noteworthy feature of the $W(CO)_4$ units is the significant deviation of the two axial carbonyl ligands from linearity. This is seen in all the dioxygen derivatives we have presently characterized (Table VIII) and may be the result of repulsion by the lone pairs on the oxygen atoms of the chelating ligands.

Relevant to the chemistry reported herein, Cooper and coworkers have observed reaction 2 to occur in nearly quantitative

$$W(CO)_5^{2-} + 2CO_2 \rightarrow W(CO)_6 + CO_3^{2-} \qquad (2)$$

yield.[15] That is, a head-to-tail coupling of two CO_2 molecules took place with formation of tungsten-bound CO and the carbonate ion, instead of a head-to-head coupling of two CO_2's to afford the oxalate ligand bound to tungsten.

Acknowledgment. Financial support of this research by the National Science Foundation (Grants 88-17873 and 91-19737) is greatly appreciated.

Supplementary Material Available: Tables of anisotropic displacement parameters, hydrogen atom coordinates, isotropic displacement parameters, and complete crystallographic data and data collection parameters for $[EtN]_2[1]$ and $[PPN]_2[2]\cdot{}^1/_2(CH_3CH_2)_2O$ (6 pages). Ordering information is given on any current masthead page.

(15) (a) Maher, J. M.; Lee, G. R.; Cooper, J. *J. Am. Chem. Soc.* **1982**, *104*, 6797. (b) Lee, G. R.; Maher, J. M.; Cooper, N. J. *J. Am. Chem. Soc.* **1987**, *109*, 2956.